ELSEVIER

Journal of Pharmaceutical and Biomedical Analysis
17 (1998) 1285–1309

JOURNAL OF
PHARMACEUTICAL
AND BIOMEDICAL
ANALYSIS

Automated system for the on-line monitoring of powder blending processes using near-infrared spectroscopy Part II. Qualitative approaches to blend evaluation

S. Sonja Sekulic [a], John Wakeman [b], Phil Doherty [c], Perry A. Hailey [c,*]

[a] *Pfizer Central Research, Groton, CT 06340, USA*
[b] *Pfizer Quality Operations, Sandwich, Kent, CT13 9NJ, UK*
[c] *Pfizer Central Research, Sandwich, Kent, CT13 9NJ, UK*

Received 8 September 1997; received in revised form 21 November 1997

Abstract

Near Infrared (NIR) spectroscopy is seen as a very powerful tool in a variety of applications involving powder characterisation. Here we deal with a typical pharmaceutical application of powder blend monitoring. A D-optimal experimental design is used to cover the 85–115% range of the target formulation which is comprised of the active component at 3.5% w/w, Microcrystalline Cellulose (Avicel PH102) at 62%, Dibasic Calcium Phosphate Anhydrous at 31.5%, Sodium Starch Glycolate (Explotab) at 2%, and 1% Magnesium Stearate. A miniature Flobin blender has been modified to enable the use of a fibre optic probe for on-line NIR spectral data collection. The experiments were successful in detecting spectral changes which eventually converged to constant variance. While the NIR spectrum of a powdered sample is rich in information which is representative of both the physical and chemical characteristics of the sample, it is at times difficult to select the appropriate mathematical treatments in order to extract the desired information. This article investigates several possible pre-treatments (including detrending (DT), standard normal variates (SNV), second derivatives, and the combination of SNV and DT) together with several ways in establishing blend homogeneity, which includes the running block standard deviation, dissimilarity calculations and principal components analysis (PCA). The focus of this work is to investigate qualitative tools of analysis for blend homogeneity determinations, while future work will focus on quantitative data interpretation.

Keywords: Near infrared spectroscopy; Pharmaceutical analysis; Blending; Process control; SIMCA; On-line analysis; Experimental design

1. Introduction

Near Infrared (NIR) spectroscopy is a powerful analytical technique with a wide array of applications in the pharmaceutical industry [1–3]. More

* Corresponding author. Tel.: +44 1304 616274; fax: +44 1304 616726; e-mail: perry_hailey@sandwich.pfizer.com

0731-7085/98/$ - see front matter
PII S0731-7085(98)00025-9

recently, considerable interest has been shown in using NIR spectroscopy for the on-line and off-line determination of powder blend homogeneity [4–7]. Part I in this series of publications describes the system design and integration. In this application of on-line blend homogeneity determination we have extended the traditional approaches by incorporating a constrained D-optimal experimental design which covers the 85–115% range of the blend components. The data set generated in this way will be used to investigate both qualitative and quantitative approaches to the data treatment. While the focus here will be on the qualitative approaches, a future publication will concentrate on the feasibility of using existing quantitative algorithms (Part III in the series).

Pharmaceutical companies devote a great deal of time, labour and equipment to the process of creating homogeneous powder blends. Blending can be described as a combination of: (i) diffusion; the redistribution of particles by the small scale 'random' movement of individual particles relative to one another; (ii) convection; the movement of groups of adjacent particles from one place to another; and (iii) shear; the change in configuration of ingredient particle locations through the formation of slip places in the mixture [4]. The ideal mix has a homogeneous distribution of all the components throughout the blender [8]. The homogeneity of a blend, in the traditional pharmaceutical sense, addresses only the distribution uniformity of the active drug substance while assuming that the excipients are also evenly distributed. The potential power of this type of on-line approach to homogeneity determinations is that the assumption of excipient homogeneity will be removed since all components of the blend mixture will contribute to the resultant NIR spectrum and are thus measured implicitly.

The role of the excipients in the final product is a significant one, in that they solubilise, flavour and fashion medicinal agents into efficacious and appealing dosage forms while also improving characteristics such as flowability and tabletting properties [9]. The typical blending procedure for formulations includes charging a blender, blending for a pre-determined length of time, stopping the blender, and manually removing samples which are representative of the blender contents. The samples are then sent to a laboratory and analysed with traditional methods such as UV/VIS spectroscopy or High Performance Liquid Chromatography. The most time consuming portion of the blending process is not the actual blending, but often the analysis that must be performed to establish homogeneity of the drug substance in the blend. This analysis is not only time consuming but may be subject to errors induced by sampling methods. The elimination of these two issues (analysis time and sampling errors) is decidedly of benefit to the pharmaceutical businesses.

A Flobin blender has been modified to accommodate a fibre optic probe which is in contact with the components being blended, and coupled to a NIR spectrophotometer. Spectral information about the formulation is collected during the blending process. This article describes the experimental design of the blender runs carried out together with the various algorithms used to evaluate the data collected. The objectives were to evaluate the information content of the data collected using qualitative approaches such as standard deviation and dissimilarity calculation, principal component analysis or model-free profiling, as well as investigating classification as a means to determine the blending end points. An additional aim is to better understand the practical implications and requirements of implementing this type of technique to routine operations within the pharmaceutical environment.

Table 1
Target formulation of the product powder blend

Name of component	Quantity, mg g^{-1} (%)
Active	34.720 (3.472)
Microcrystalline cellulose (Avicel)	620.380 (62.028)
Dibasic Ca phosphate anhydrous (DCP)	315.000 (31.500)
Sodium starch glycolate (Explotab)	20.000 (2.000)
Magnesium sterate	10.000 (1.000)

Table 2
Experimental design of blend components each covering the 85–115% of the target formulation range (exculding Avicel which is used as a filter in the design)

Exp. no.	Exp. name	Run order	Active	Avicel	DCP	Explotab
1	B1	10	0.0333334	0.679667	0.27	0.017
2	B2	17	0.0366667	0.676333	0.27	0.017
3	B3	19	0.0333334	0.673667	0.27	0.023
4	B4	15	0.0366667	0.670333	0.27	0.023
5	B5	11	0.0333334	0.583667	0.366	0.017
6	B6	2	0.0366667	0.580333	0.366	0.017
7	B7	13	0.0366667	0.574333	0.366	0.023
8	B8	7	0.0333334	0.577667	0.366	0.023
9	B9	18	0.03[a]	0.571	0.366	0.023
10	B10	3	0.04	0.673	0.27	0.017
11	B11	9	0.04	0.577	0.366	0.017
12	B12	1	0.04	0.667	0.27	0.023
13	B13	12	0.03	0.681	0.27	0.019
14	B14	8	0.03	0.583	0.366	0.021
15	B15	14	0.03	0.651	0.302	0.017
16	B16	4	0.03	0.613	0.334	0.023
17	B17[b]	20	0.035	0.627	0.318	0.02
18	B18[b]	16	0.035	0.627	0.318	0.02
19	B19[b]	6	0.035	0.627	0.318	0.02
20	B20[b]	5	0.035	0.627	0.318	0.02

[a] According to design should be 0.04, but 0.03 actual weight used.
[b] Target composition.

2. Experimental

The target formulation for this product and investigation is given in Table 1. All the spectral data collected in this study was completed prior to the addition of magnesium stearate. The experimental design, manufacturing process and instrument set-up are discussed in more detail below.

2.1. Experimental design of blends

Classical experimental designs, such as factorial designs are well known but often require a large number of experiments. Furthermore they are inappropriate for mixture designs where the experimental region is constrained or irregular. One approach to developing calibration sets from a list of possible experiments is to use the D-optimal criteria. This involves selecting a number of samples that maximise the determinant of $(X^{T}X)$. Here, a constrained D-optimal mixture design has been employed. All components within the formulation, excluding microcrystalline cellulose, have been varied from 85–115% of intent. The microcrystalline cellulose is used as a filler to ensure total composition sums to unity. The experiments obtained with this design are listed in Table 2, which shows the randomisation of the blend runs and the individual component compositions.

2.2. Manufacturing process

The manufacturing process for the Product blend can be described as having two phases and is shown graphically in Fig. 1. Phase I consists of the initial charging and mixing of blend components for a period of 5 min. At the end of this phase the blend mixture is transferred into a Fitzmill and undergoes a milling step (Speed: Medium, Knives: Forward). At the completion of the milling step, the mixture goes through a sieve step (Screen 24183) with the purpose of nominally delumping the contents. The mixture is then returned to the Flobin and Phase II (or post-screen) blending is resumed for an additional 25 min.

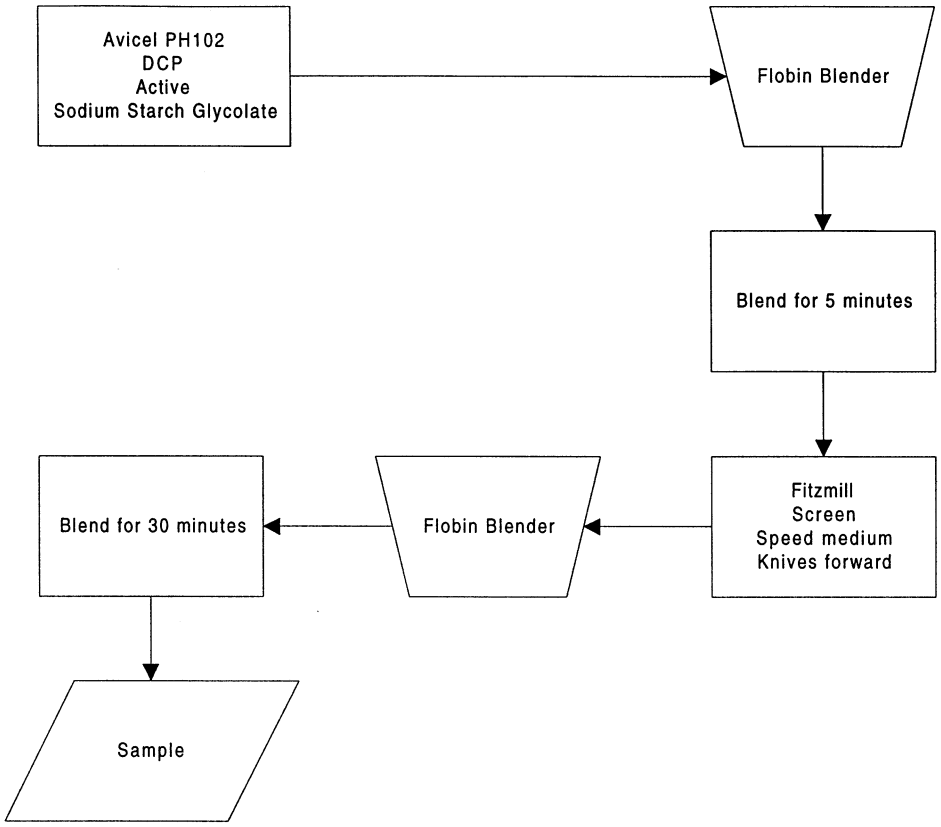

Fig. 1. Flow diagram of the blending process.

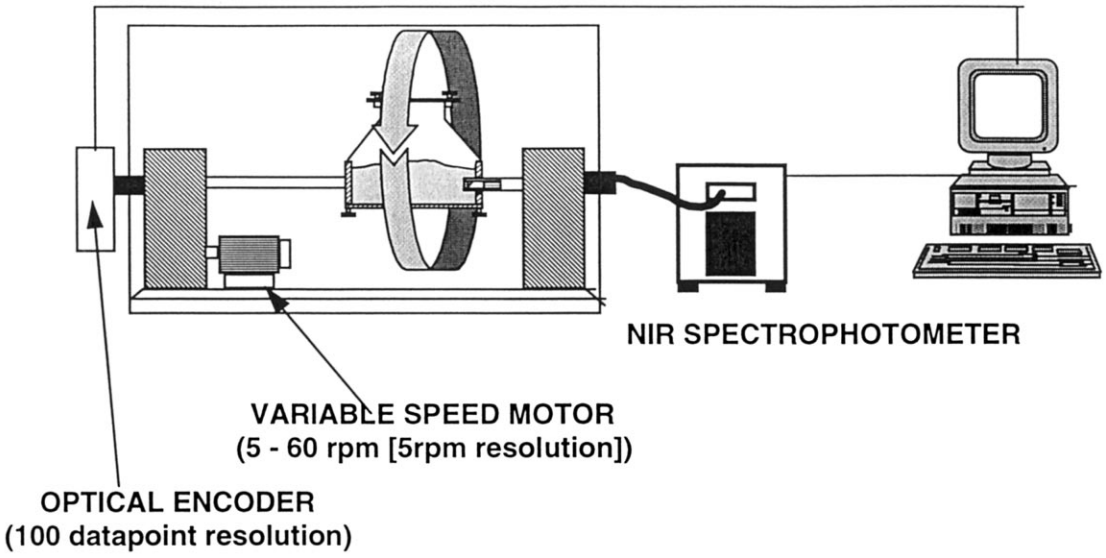

Fig. 2. Instrument and blender operating configuration.

2.3. Instrumentation

The automated on-line blender system employs a NIRSystems 6500 monochrometer (NIRSystems, Silver Spring, MD) for spectral acquisition. The spectrophotometer is coupled to the blending vessel by means of a fibre-optic which is housed in a bearing. The bearing has been suitably engineered to allow the blender to rotate while the fibre-optic itself remains stationary. For the Flobin blender this equates to a rotational point from one top corner to the diagonally opposite top corner. An optical shaft encoder reports the position of the blender to a custom built electronic interface device by utilising a zero datum pulse from the encoder. This rotational position is then converted into a seven bit binary format and output to the digital I/O board in the control PC via the parallel port. The PC sends control commands to the electronic interface to start and stop blender rotation and instruct the motor to rotate at the one of 12 pre-set rotational speeds (5–60 rpm). The spectrophotometer and blender set-up are shown in Fig. 2. The rotational speed of the blender selected for this study was 10 rpm. The spectral acquisition is triggered from the LabView software via dynamic data exchange (DDE) communication with the spectrophotometer WINSAS software. More specific details of the instrument/blender interface can be found in reference [5].

2.4. Spectral acquisition

The on-line spectral data acquisition using the fibre-optic probe configuration was operated in a discrete stop-start mode such that spectral acquisition was triggered only when the blender was stationary. A total of 20 scans were co-added to produce the final spectrum covering the wavelength range 1100–2500 nm at 2 nm intervals. One spectrum was collected immediately after the blender was charged with the individual components. At each time point after that, the blender was stopped, three separate spectra were collected, each after a single rotation of the blender. The blender rotation was restarted until the next spectral acquisition point. During the spectral acquisition, the blender was in an inverted position which is shown in Fig. 3. The time interval between triplicate scans, varied depending on the

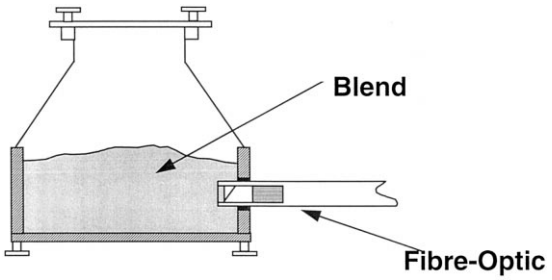

Fig. 3. Fibre-optic probe interface with the Flobin blender.

Table 3
Time sequence describing the points at which the spectral data was collected

Time (s)	No. of scans	Total processing time (s)
0	1	0
30	3	30
60	3	60
90	3	90
120	3	120
150	3	150
180	3	180
210	3	210
240	3	240
270	3	270
300	3	300
Post-screen	1	300
30	3	330
60	3	360
90	3	390
120	3	420
180	3	480
240	3	540
300	3	600
360	3	660
420	3	720
480	3	780
540	3	840
600	3	900
720	3	1020
840	3	1140
960	3	1260
1080	3	1380
1200	3	1500
1320	3	1620
1440	3	1740
1560	3	1860
1680	3	1980
1800	3	2100

stage of the blending process. As shown previously in Fig. 1, the blending process is undertaken in two phases. During Phase I, the time interval is 30 s between triplicate scans. After the screening step, an initial scan is taken once, and then the triplicate scans are resumed for the remainder of the blending time. The time interval between triplicate scans increases as the blending proceeds. The total number of spectra collected in this way was 98 per blending experiment. The actual spectrum collection time points are listed in Table 3. The Total Processing Time (listed in column 3 of Table 3) was used as the reference time axis for all the batch comparisons as it is representative of the entire processing time.

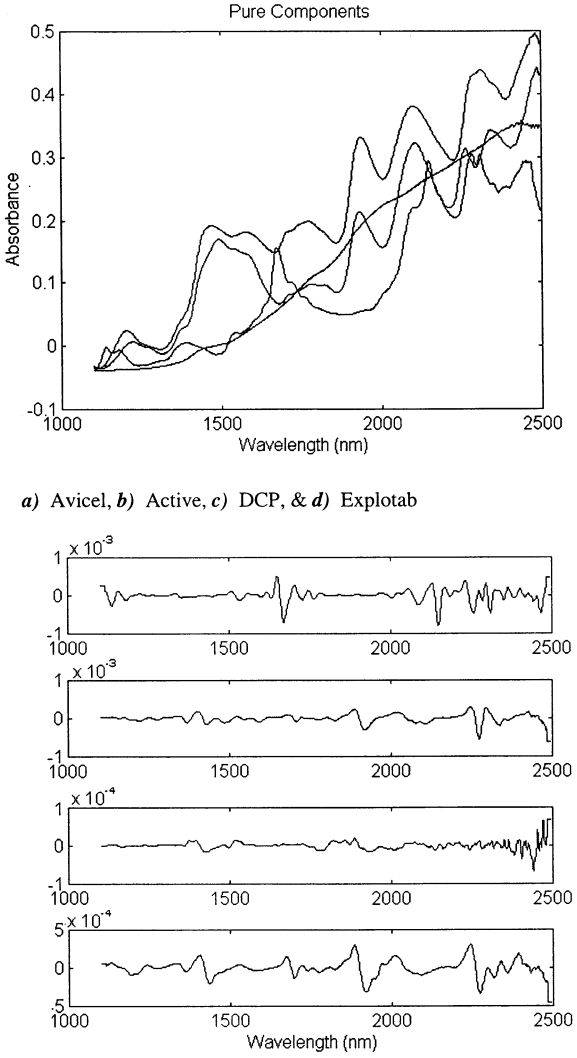

a) Avicel, *b)* Active, *c)* DCP, & *d)* Explotab

Fig. 4. NIR spectral data of formulation components.

In addition to the spectral data collected during the designed blend runs, NIR spectra were collected on the individual blend constituents. The typical spectrum obtained in this way is shown in Fig. 4. This figure shows both the raw spectral data and the individual components after a second derivative transform has been applied in order to show some of the spectral differences which are more difficult to see in the raw spectral format.

2.5. Software

Several software packages have been used throughout this work, starting with LabView version 3.1 for instrument control (National Instruments, Austin, TX), Winsas version 1.09 for spectral data acquisition (NIRSystems, Silver Spring, MD), the constrained D-optimal experiments were designed using Modde for Windows, Version 2 (Umerti, Sweden). The data analysis was carried out in Matlab, Version 4.21c (Mathworks, Natick, MA) and also Piroutte, Version 1.21 (Infometrix, Seattle, WA). In addition to the two data analysis packages used, Masterkey version 1.00 (Infometrix, Seattle, WA) was used for file format conversion from Winsas to a flat-ASCII format suitable for both Matlab and Pirouette.

3. Data analysis

The term data analysis is used to cover multiple activities including the mathematical pre-treatments or transforms performed on the collected spectral data prior to any data interpretation as such. Depending on the purpose of the application, the user may or may not be interested in the spectral contributions originating from the physical characteristics of the sample. Where these characteristics are important, the user may choose to work with the raw spectral data, otherwise some pre-treatment or pre-processing is usually carried out. The sections below briefly describe

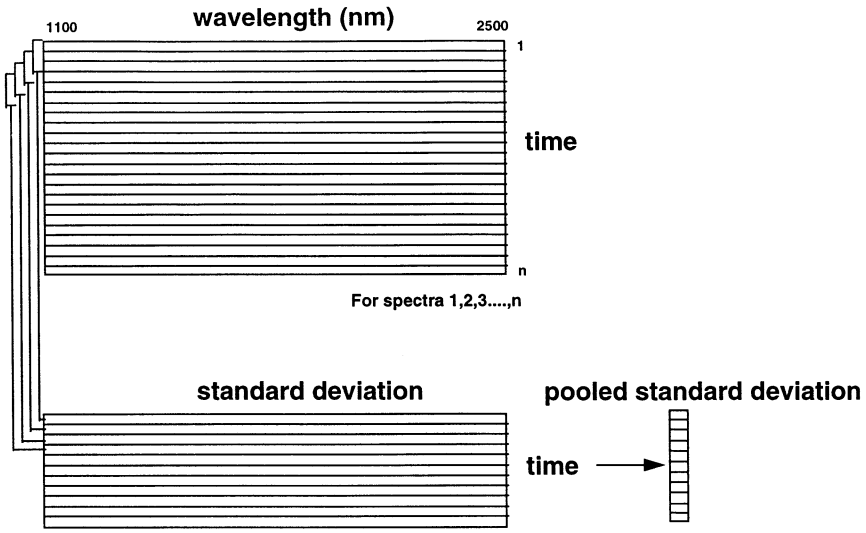

Fig. 5. Graphical representation of the moving block standard deviation calculation for blend homogeneity evaluation.

the pre-processing options incorporated into this study, together with the algorithms used to evaluate the blend homogeneity after the selected pre-processing is carried out.

3.1. Spectral pre-processing

3.1.1. Raw spectral data

Even though an exorbitant amount of effort is directed toward the evaluation of appropriate pre-processing techniques and algorithms which pertain to NIR spectroscopic data, there are still a significant number of applications where inspection of the raw spectral data may be very informative. Specifically in blend homogeneity determinations where both the physical and chemical characteristics of the blend components can provide useful information in establishing or evaluating blend homogeneity. Calculations on raw spectral data are therefore included here as one of the viable options for data interpretation.

3.1.2. Detrending (DT) [10]

The simplest forms of spectral pre-processing aim at corrections for baseline differences. This includes both linear offsets or, as is the case with NIR spectroscopy, non-linear approximations of the baseline. The DT transformation is in essence a quadratic baseline correction. The spectra are fitted to a quadratic function which is then subtracted from the original spectrum.

$$x_{i,k}^{\mathrm{DT}} = x_{i,k} - \tilde{x}_{i,k} = x_{i,k} - (a + b \cdot k + c \cdot k^2) \qquad (1)$$

Here, a, b and c are constants, i is the spectrum index, k is the wavelength index. The quadratic approximation of Eq. (1) is then subtracted from the original spectrum. The corrected spectra have zero mean and non-zero variance. This pre-processing strategy is applied to individual spectra, i.e. the baseline correction is calculated for every spectrum individually.

3.1.3. Standard normal variates (SNV) [10]

Another quite popular way of dealing with the baseline is to perform one of the many mean-centring operations available. The SNV transformation is slightly different in that it requires that the mean of the individual spectrum data points ($\bar{x}_i$) be subtracted from the spectrum and then divided by the standard deviation (s_i) of the same spectrum (Eq. (2)).

$$x_{i,k}^{\mathrm{SNV}} = (x_{i,k} - \bar{x}_i)/s_i \qquad (2)$$

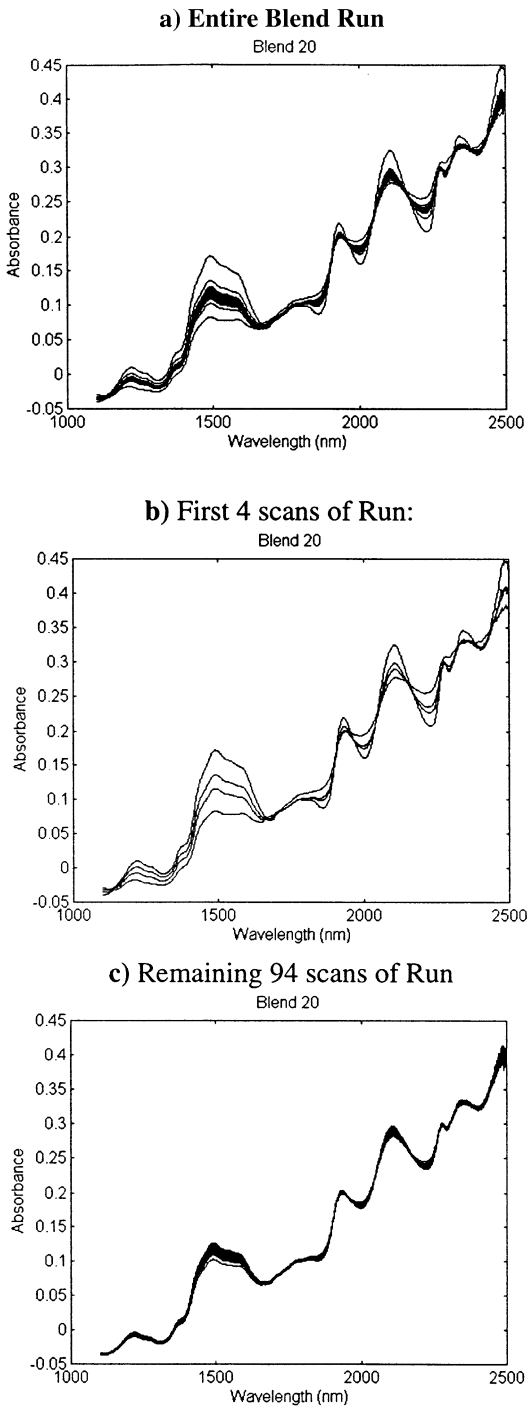

Fig. 6. NIR raw spectral data of Blend # 20. (a) Entire blend run. (b) First four scans of run. (c) Remaining 94 scans of run.

The corrected spectra have zero mean and variance equal to one. The advantage of an approach like SNV is that the transformation is applied to individual spectra rather than the mean calculated for a group of spectra.

3.1.4. Second derivatives

Although several types of derivatives are possible, in practice the second derivative is encountered more often than not when dealing with NIR spectroscopic data. The advantage of using the second derivative is that both the offset and drift components of the spectra, due to the physical nature of the sample, are minimised. A second derivative calculation, in this case a Savitzky-Golay [11] variation, was employed. In this way the spectral contributions resulting from the physical properties of the sample are effectively handled.

3.1.5. Standard normal variates (SNV): detrending (DT)

Since the SNV transformation deals only with the baseline offset but not the curvature of the baselines encountered with NIR reflectance spectroscopy, it was decided to couple the SNV and DT transformations. In this way, both the offset and curvature of the baselines would be handled and would serve as a good comparison to the second derivative approach to pre-processing.

3.2. Batch profiling tools

3.2.1. Mean standard deviation versus blend time

The most intuitively obvious way to evaluate the rate of change of a process is to calculate the standard deviation over some interval of that process. As the process becomes more stable or reproducible, the standard deviation would approach zero. With a multivariate process measurement such as NIR spectroscopy, the above concept can be modified to accomplish essentially the same task. First, a window size is selected to encompass a sufficient amount of information with which to evaluate the state of the process without diminishing the information content by making the window too large. The standard deviation of the absorbance for each wavelength is calculated over the nine spectra, resulting in a

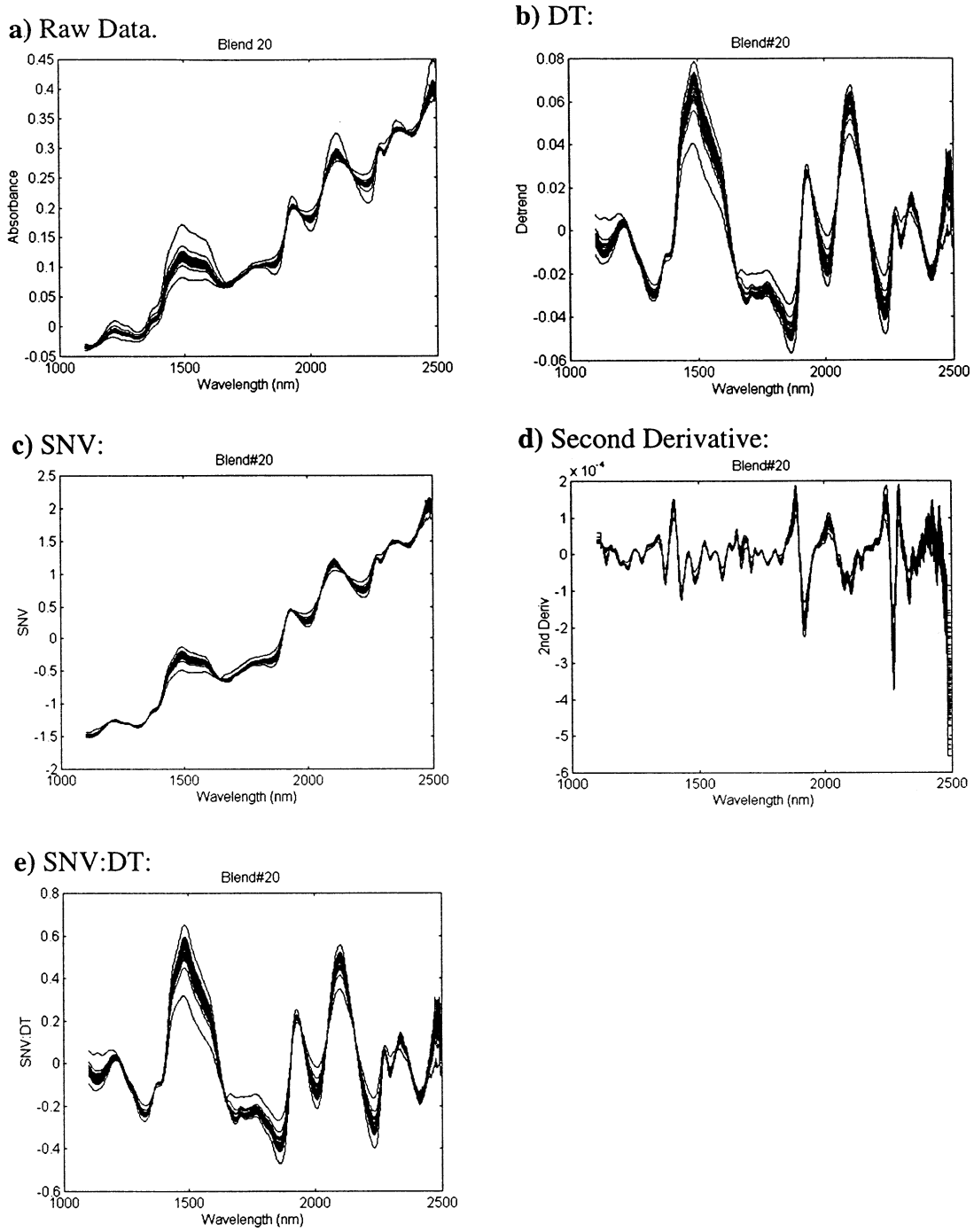

Fig. 7. Examples of spectral pre-processing with Blend # 20. (a) Raw data; (b) DT; (c) SNV; (d) Second derivative; (e) SNV:DT.

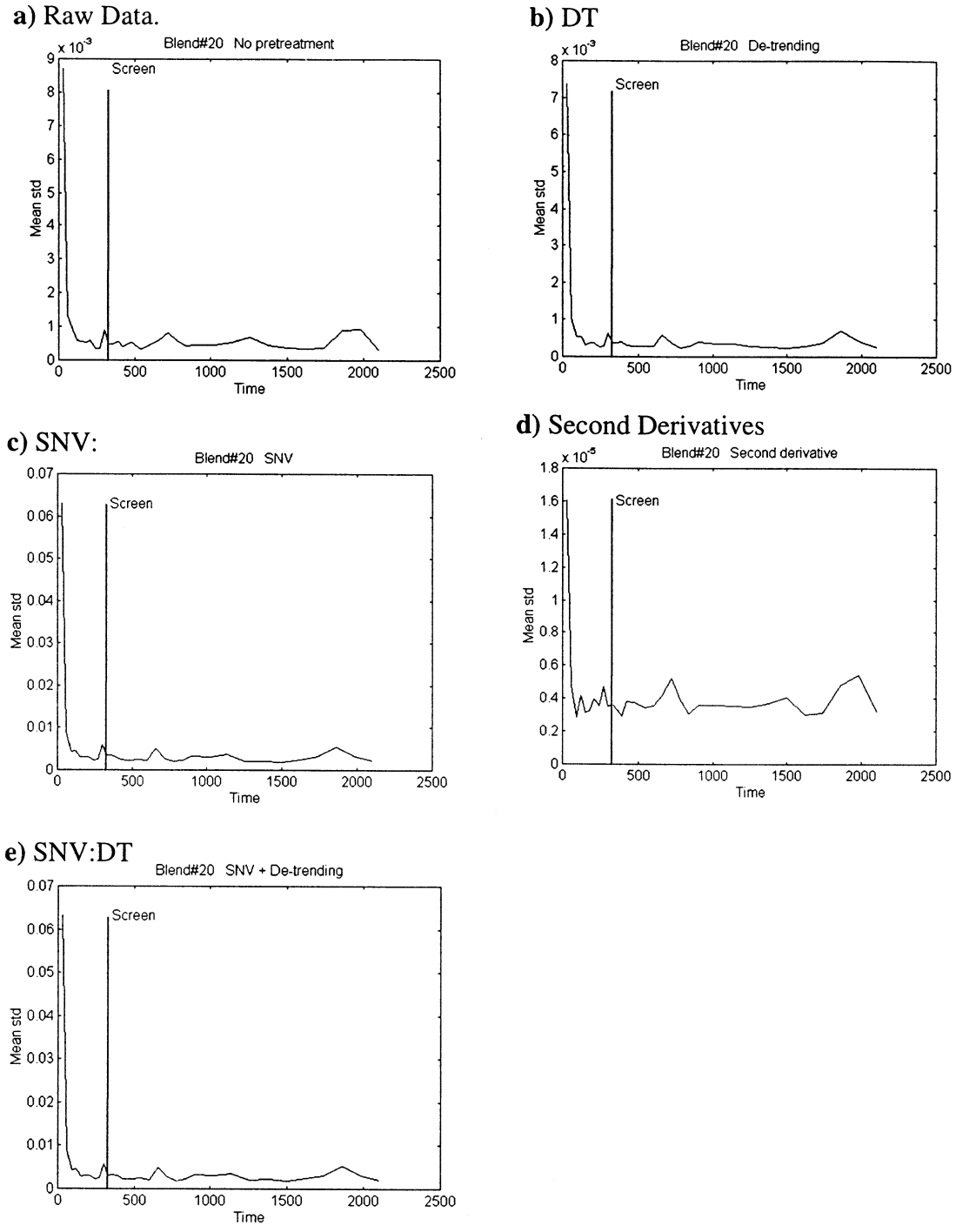

Fig. 8. Examples of blend homogeneity evaluation using the mean standard deviation with Blend # 20 (wavelength range used: 1100–2500 nm). (a) Raw data; (b) DT; (c) SNV; (d) Second derivative; (e) SNV:DT.

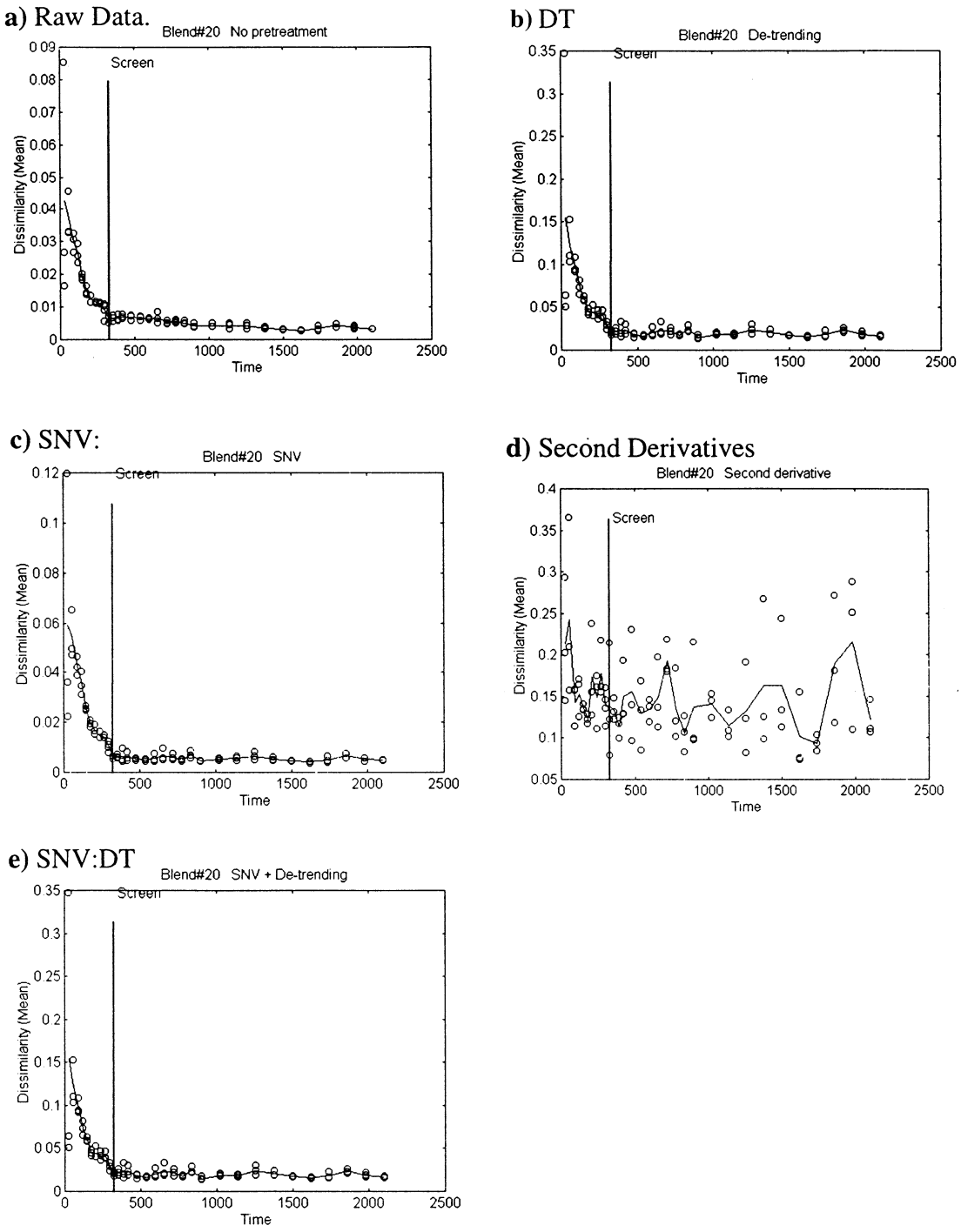

Fig. 9. Examples of blend homogeneity evaluation using the dissimilarity calculated against a target spectrum (times = 1620, 1740 and 1860 s) with Blend # 20 (wavelength range used: 1100–2500 nm). (a) Raw data; (b) DT; (c) SNV; (d) Second derivative; (e) SNV:DT.

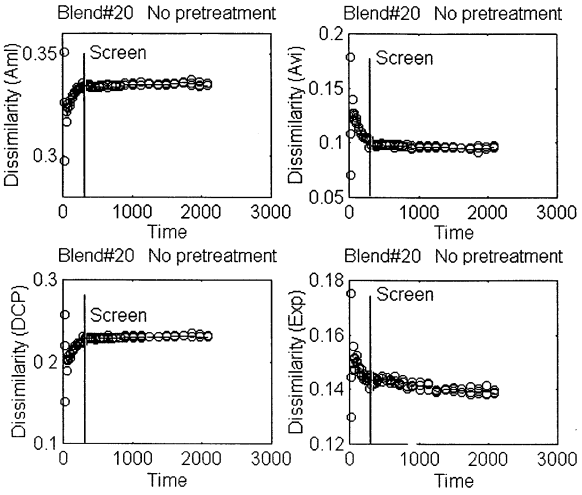

Fig. 10. Dissimilarity of Blend # 20 with the pure component spectra (wavelength range used: 1100–2500 nm).

standard deviation spectrum. The pooled standard deviation (over all wavelengths) of the standard deviation spectrum is reported as a single value. The process is actually depicted graphically in Fig. 5. The mean standard deviation is then plotted against the process or blending time.

3.2.2. Dissimilarity versus blend time

The ideal application would be to calculate a theoretical target spectrum from the individual component spectra and calculate the dissimilarity of the on-line spectra in real time compared to the theoretical target spectrum. In practice, this concept is difficult to achieve since the mixing of different powder constituents does not conform to the linear additivity requirement, i.e. the sum of the individual component spectra does not equal the mixture spectrum. There are two slightly more practical ways of evaluating the similarity or dissimilarity of a target spectrum.

3.2.2.1. Dissimilarity of individual spectra when compared to an average set of scans considered to have reached homogeneity. This deals with the sample matrix as an entity rather than dealing with the individual components of the mixture. Conceptually this is a very feasible approach, that has a lot of potential for being applied dynamically. However, the target spectra (or spectrum) need to be collected prior to a blend run in order to have the capability of calculating spectral dissimilarity in real-time. In practical terms this generally means that one blend run needs to be sacrificed in order to collect the target spectra, thereafter applying the analysis dynamically. Alternatively, if equivalence can be established between a small scale synthetic mix of the appropriate composition and the full-scale 'real' blend mixture, the possibility exists of pre-determining the target spectrum. This approach would enable the user to collect the target spectrum ahead of time and thus make possible dynamic homogeneity evaluation from the first run. To date, there have been no literature reports on scale up of blending processed using NIR spectroscopy.This is currently under investigation in this laboratory.

3.2.2.2. Dissimiarity of indivdual spectra when compared to indiviual pure component. As previously stated, the traditional approach focuses completely on the active drug component of the blend mixture for the determination of homogeneity. While this approach is widely accepted, the extent of mixing of the remaining components could have significant impact on the tabletting or dissolution properties for example. The calculation of the extent of dissimilarity of a spectrum collected during a blend run when compared to the spectra of the individual components can provide insight into the extent of homogeneity for each of the individual components in the mixture. The advantage of this type of approach is that spectra on the pure individual blend components can be collected quickly and easily prior to any full-scale blending runs, after which dynamic evaluation of extent of homogeneity can be carried out. The dissimilarity is calculated by normalising the spectra collected during the blender run ($x_{i,k}$), as well as either the target spectra ($t_{i,k}$) of the pure component spectra ($p_{i,k}$) to unit length. The normalised blend spectra ($x^N_{i,k}$) are then projected orthogonally onto the normalised target spectra, $t^N_{i,k}$ (or pure spectra, $p^N_{i,k}$) using the Gram-Schmidt orthogonalisation procedure [12] (Eq. (3)).

$$Diss_i = x^N_{i,k} - (x^N_{i,k} \times (t^N_{i,k})^T) \times t^N_{i,k} \quad (3)$$

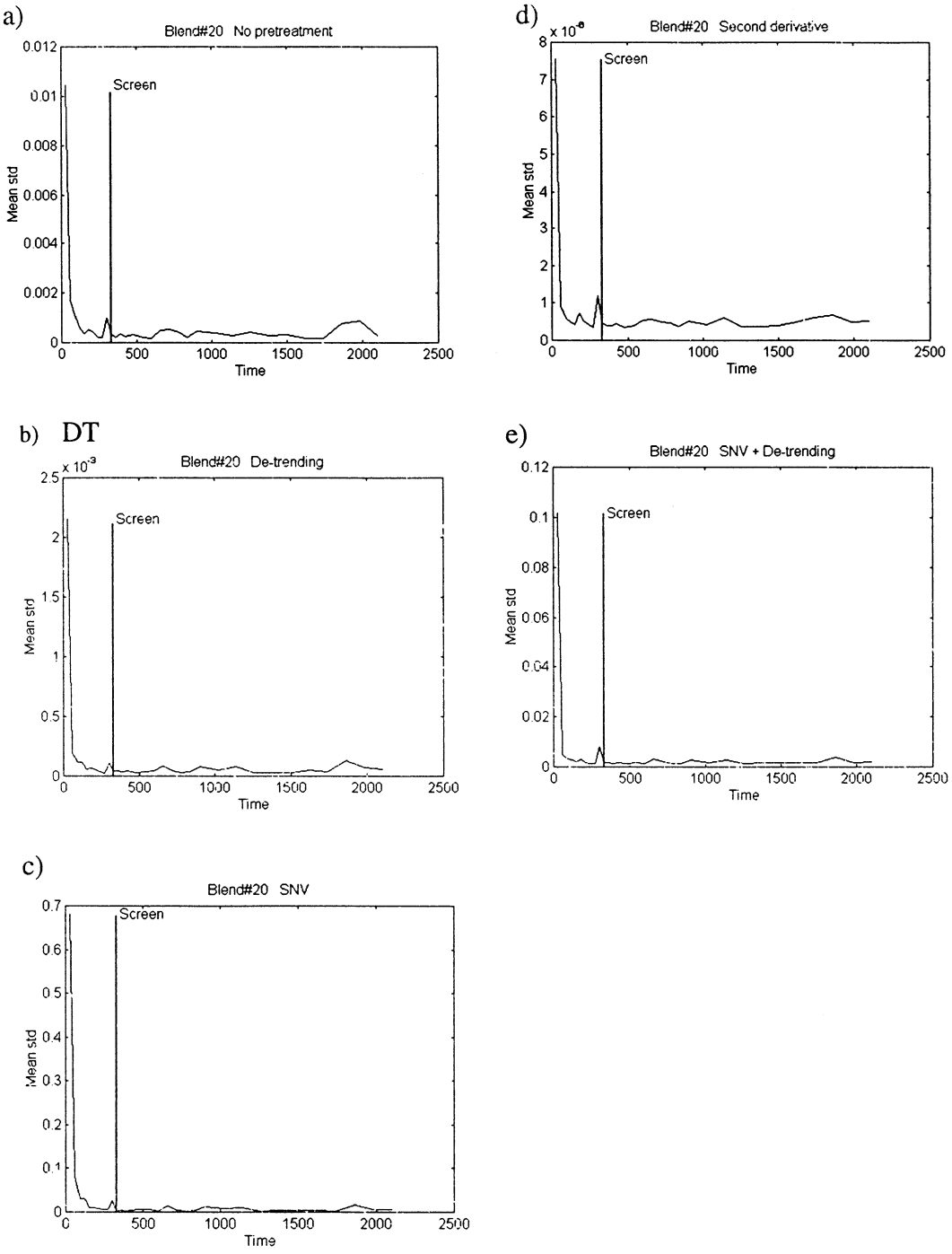

Fig. 11. Blend # 20 evaluation with the moving block standard deviation calculation over the wavelength range 1500–1800 nm.

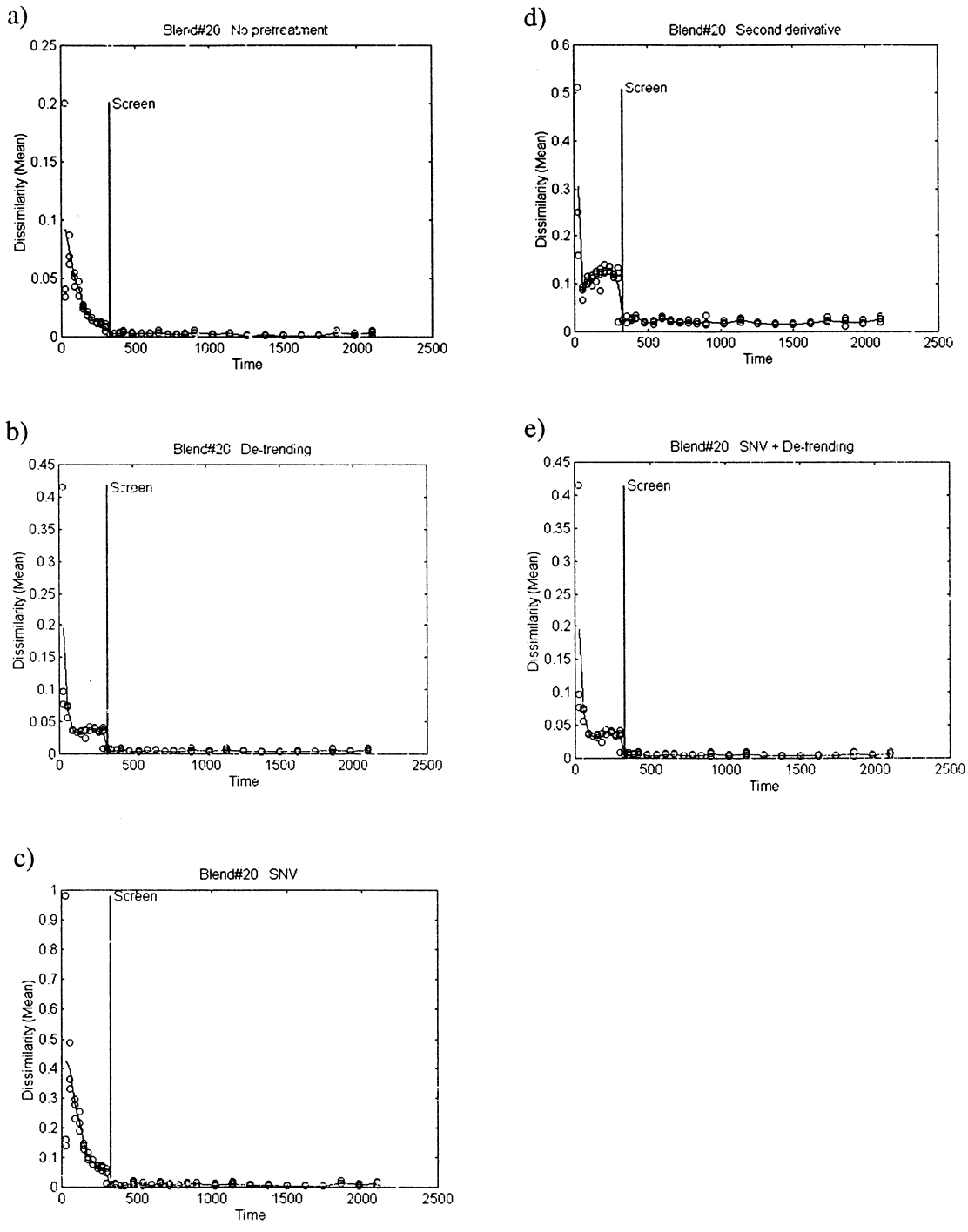

Fig. 12. Examples of Blend # 20 evaluation with a variety of pre-processing options (wavelength range use: 1500–1800 nm).

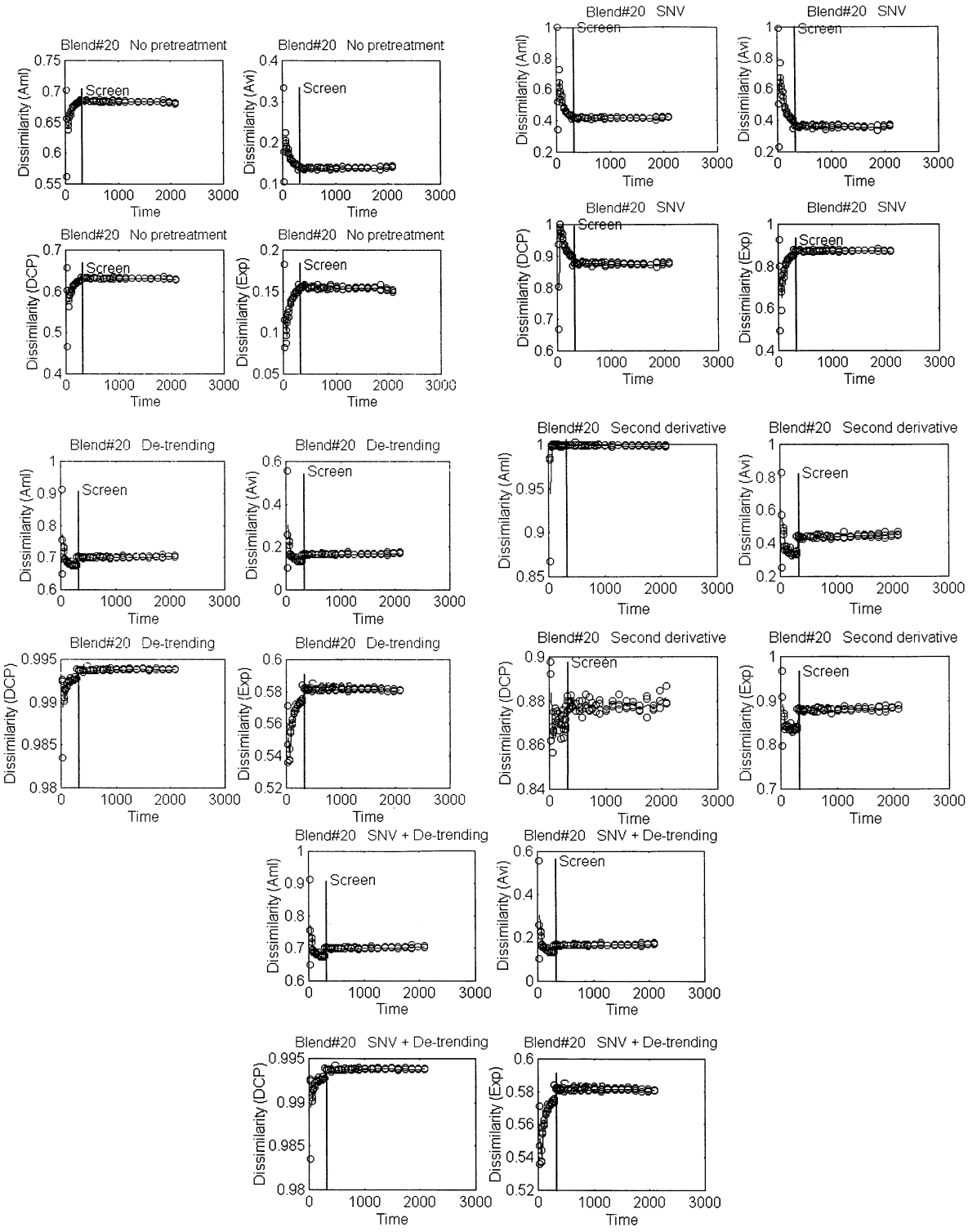

Fig. 13. Dissimilarity calculation with respect to the individual component pure spectra with a wavelength range of 1500–1800 nm with the listed pre-processing transformation.

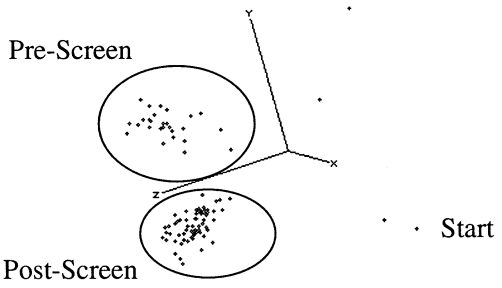

Fig. 14. Principal component plot of Blend # 20 plotted in the space defined by the first three principal components (second derivative transform, 1100–2300 nm).

The length of the vector orthogonal to the target spectrum is used as a measure of dissimilarity. The calculated dissimilarity values are plotted against blend time and the profiles examined for steady state conditions which would indicate that the process has reached homogeneity.

3.2.3. Principal component analysis (PCA) [13]

Generally considered to be a retrospective form of analysis since the decomposition needs to be performed on the entire set of spectra collected during a blend run. However, it is included here as it is considered to be a tool for qualitative analysis which does not require a reference technique to be used.

The algorithm used for this calculation is based upon the Singular Value Decomposition algorithm contained in MATLAB. Consider the matrix X (dimensions $i \times k$) which contains the collected NIR spectra arranged in rows such that each row represents one time point in the blend monitoring process. The matrix X is then decomposed into three matrices (Eq. (4)):

$$X = USV^T \tag{4}$$

where U represents the scores, S is a diagonal matrix of the square root of the eigenvalues of X^TX and XX^T, V contains the loadings and T indicates the transpose. The values in the S matrix are ordered such that $s_1 > s_2 > ... > s_n$, i.e. the first principal component describes the direction of

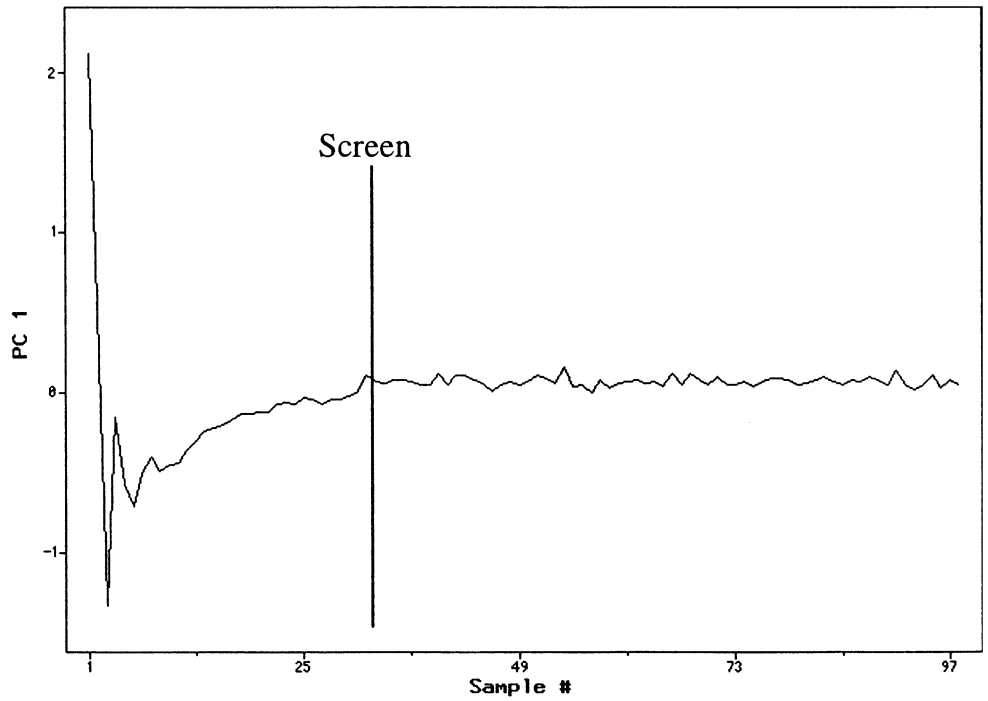

Fig. 15. Plot of the first principal component score vector against the sample number (corresponds to spectrum number), after a second derivative transform over the 1100–2300 nm range.

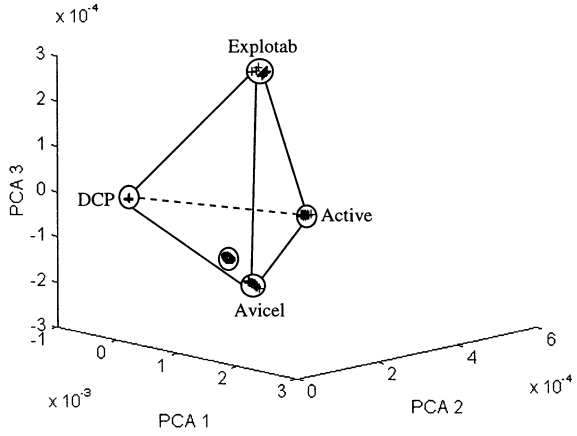

Fig. 16. PCA plot of the designed experiment spectra decomposed with replicate scans of the individual pure components projected into a space defined by the first three principal components.

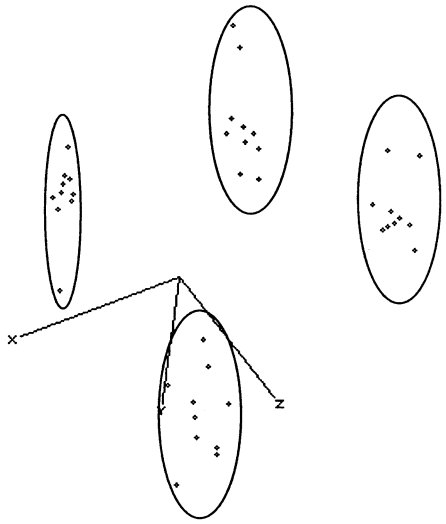

Fig. 17. PCA plot of the four target blend runs (second derivative transform over 1500–1800 nm) projected into the space defined by the first three principal components.

greatest variance encountered in the response space, the next principal component describes the next greatest amount of variance and so on.

3.2.4. Guided principal component analysis (G-PCA)

Once again, this type of analysis is done retrospectively. Conceptually this is exactly the same as regular PCA, however, by including the pure component spectra in the data set, the PCA decomposition is in effect being guided by the extremum points which are the pure components of the mixture. These extremum points would define all the possible mixtures of the individual components with the target formulation which would be located at a distance proportional to the concentration of the individual extremum point component. Once again, since linear additivity is rarely observed in practice for powder systems, this concept does not hold mathematically and can generally only be used as a guide. This will be investigated in more detail in the quantitative section of this work and will not be discussed in more detail here.

3.2.5. Soft independent modelling of class analogy (SIMCA)

The goal of SIMCA is reliable classification of unknown samples. This is accomplished by performing measurements on a set of training samples and creating a principal component model for each class in the set. For blend monitoring purposes, the procedure would be to identify the target spectra which define the blending end point and construct a SIMCA model on that set of spectra. The object is to then monitor the progress of a blend and compare the individual scans during the blend run with the cluster of target spectra used for the SIMCA model. In theory, the blend end point cluster will be consistent from run to run, but in practice this would need to be investigated and confirmed.

The SIMCA approach requires that a PCA decomposition is performed for each class of compounds in the calibration or training set of samples which contain the target blend spectra. For any one class, construct a model based on n principal components, such that T_n contains the score vectors and L_n contains the n loading vectors (Eq. (5)).

$$\tilde{X} = T_n L_n^T \tag{5}$$

The n principal components are used to reconstruct the matrix X containing the desired spectra. After the reconstruction, the difference between the original and reconstructed matrices can be calculated according to (Eq. (6)):

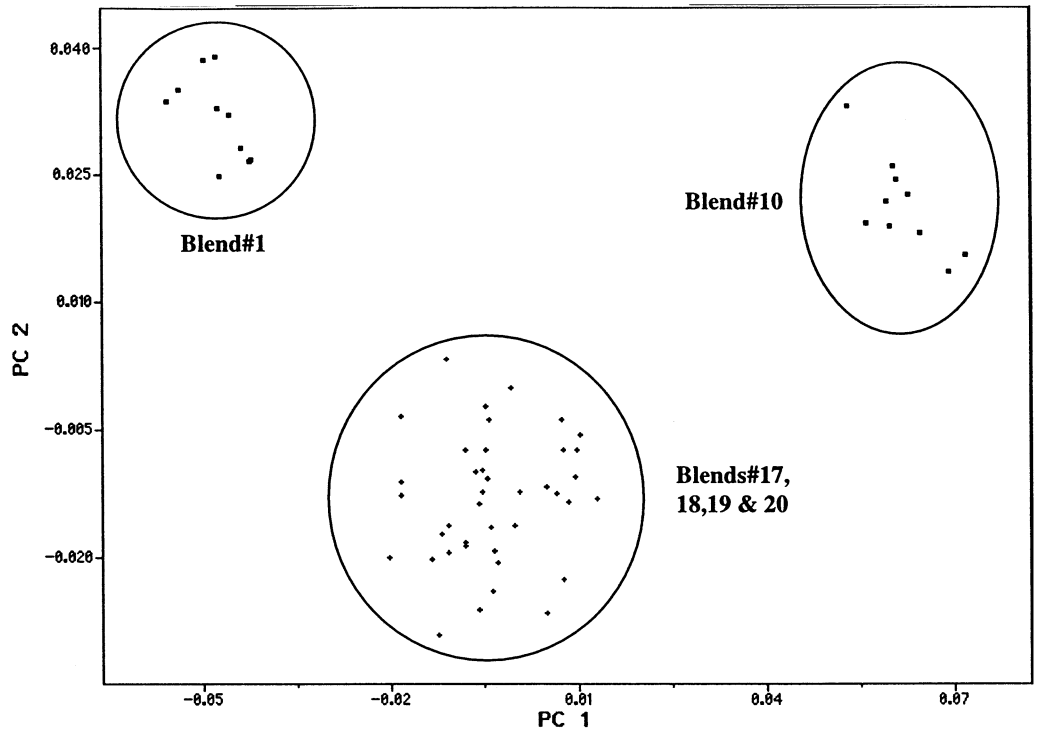

Fig. 18. PCA plot showing Blend # 1 and Blend # 10 compared against the four replicate target blends (17, 18, 19 and 20).

$$\epsilon = X - \tilde{X} = X - T_n L_n^T \tag{6}$$

The residual variance of the target class is therefore (Eq. (7)):

$$S_0^2 = \sum_i \sum_k \frac{(\epsilon_{i,k})^2}{((i-n-1)(k-n))} \tag{7}$$

where, i indicates the number of samples in the class, k is the number of variables or wavelengths and n is the number of principal components used in the reconstruction of X.

For each scan collected during the blending process, the measured response (in this case the spectrum) of the sample is projected onto the eigenvectors of the class, and thus the sample score vector is calculated (Eq. (8)):

$$\tilde{t}_u = x_u L_u \tag{8}$$

where, x_u is the spectrum and $\tilde{t}_u$ is the score vector (the sample's new coordinates on the eigenvector axes) of sample u. It is now possible to calculate the difference of the reconstructed spectrum ($\tilde{x}_u = \tilde{t}_u L_n^T$) with that of the original raw spectrum (Eq. (9)):

$$\epsilon_u = x_u - \tilde{t}_u L_n^T \tag{9}$$

This enables the calculation of the sample residual variance (Eq. (10)):

$$s_u^2 = \sum_i \sum_k \frac{(\epsilon_{(u)i,k})^2}{(k-n)} \tag{10}$$

An F-test is then used to test the hypothesis that the sample residual variance is significantly different from the target class residual variance, or not, according to (Eq. (11)):

$$s_0^2 = \sum_i \sum_k \frac{(\epsilon_{i,k})^2}{((i-n-1)(k-n))} \tag{11}$$

If the blend sample variance is found to be significantly different, the sample does not belong to the target class. However, if the sample is not significantly different, it is assumed to belong to that class and the blend is considered to be homogeneous. Note that all the F-tests are performed at a pre-defined and specified confidence level.

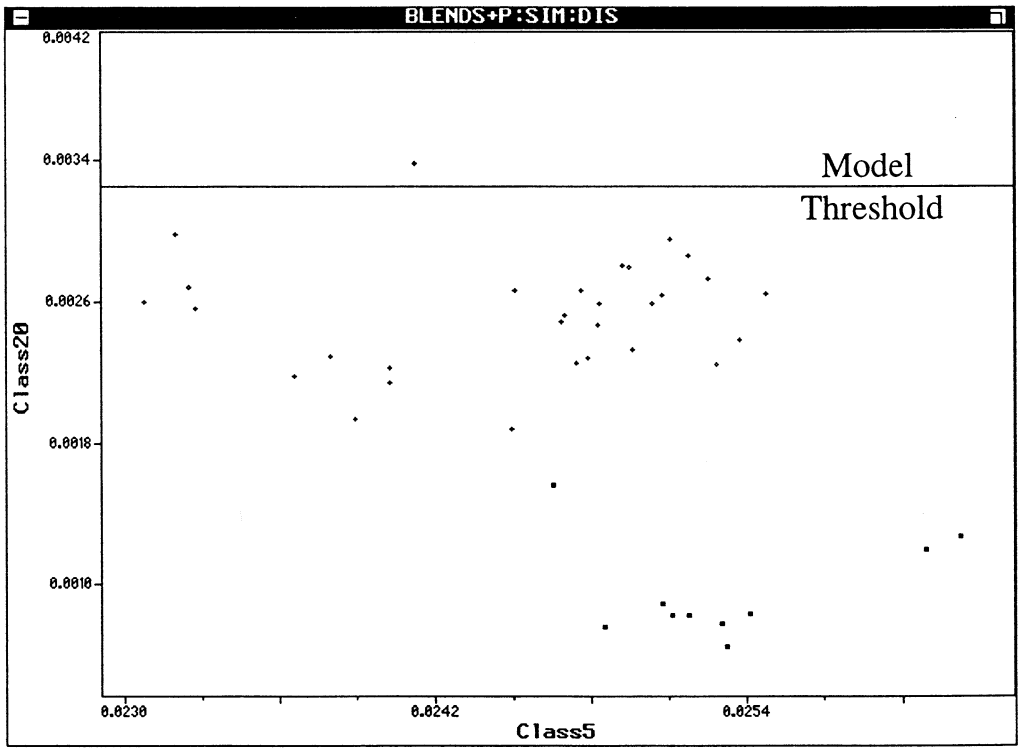

Fig. 19. SIMCA model prediction of the four target blend runs.

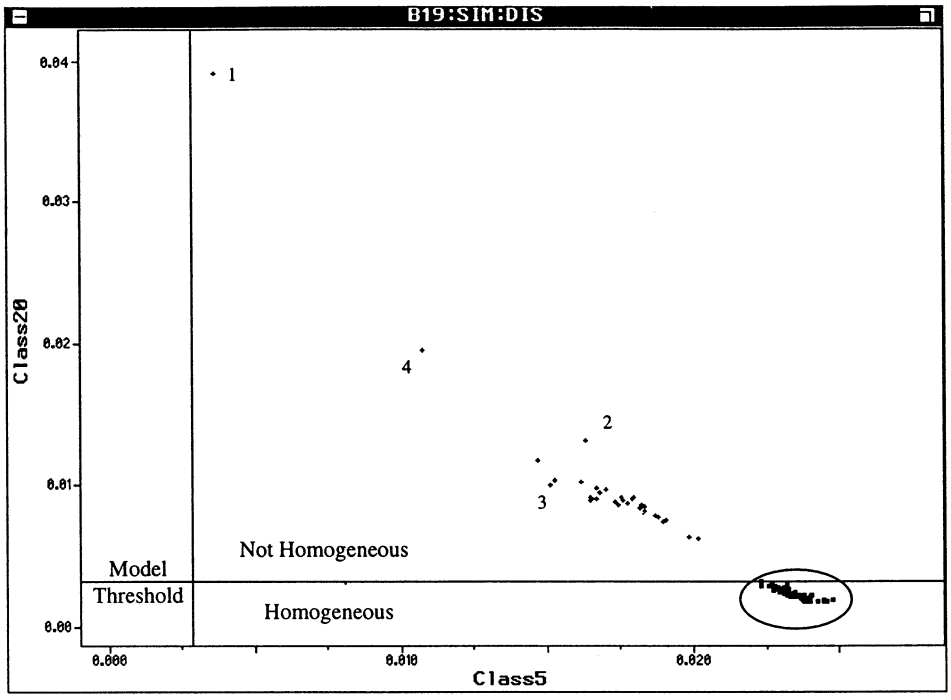

Fig. 20. SIMCA prediction of Blend # 19 with a model constructed from the blend endpoint for Blend # 20 using one principal component.

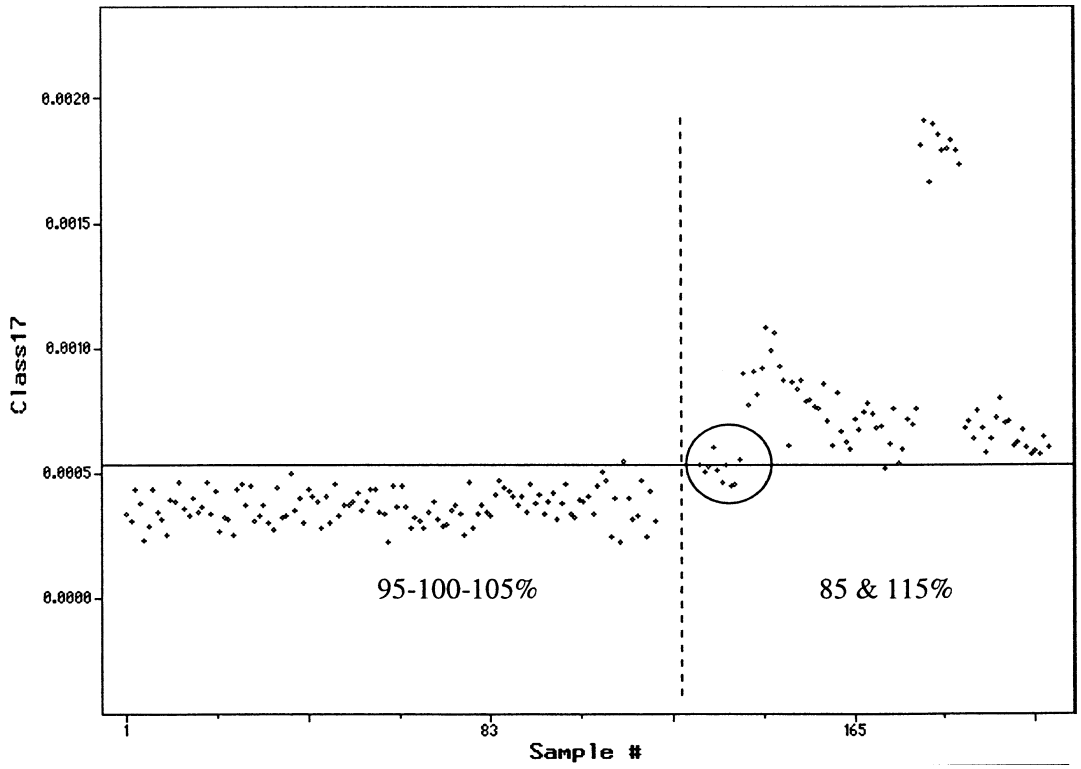

Fig. 21. SIMCA distance plot for model constructed using Active data 95, 100 and 105% of target composition, predicting the calibration data followed by the 85 and 115% of target data.

4. Results and discussion

4.1. Spectral pre-processing

A total of four blend runs were carried out with the target formulation. As an example of a target blend formulation Blend # 20 was selected to show the typical responses observed throughout the study which incorporated a total of 20 designed blends. One of the first observations is shown in Fig. 6 where the raw spectral data is plotted over the entire wavelength range of 1100–2500 nm. Part (a) of the figure shows the spectral data collected over the entire blend run, part (b) shows that the majority of the observable change occurs during the first four scans, while the last portion of the figure demonstrates a significantly smaller visual difference in the remaining 94 spectra collected during the run. It is however, unlikely that the blend is homogeneous after only 30 s of blending. This demonstrates the need for further mathematical pre-processing of the collected spectral data.

The same test case, Blend # 20, is used to contrast the pre-processing algorithms listed above, with the resultant spectra shown in Fig. 7. With all the pre-processing algorithms, the raw spectral observation is confirmed in that the greatest amount of variability is observed with the first four scans collected during the run. This is also observed for the other 19 blender runs in the study. Most blends will be stratified at the beginning of the blending process as a result of the charging procedure whereby the probe is likely to be exposed to only one of the blend components. The other observation is that the transformed second derivative spectra have an observably greater noise contribution in the 2300–2500 nm wavelength range. This too is an expected result based on previous studies and is easily confirmed

by visual inspection. Note the different scaling on the y-axis that results from the different pre-processing algorithms and closer examination of the remaining transforms also shows an increase in noise in the same region. All the transforms accomplish their respective tasks, and at this stage it is not possible to evaluate the utility of one against the other without looking at the blend profiles.

4.2. Blend profiling

In order to evaluate the utility of the pre-processing algorithms, it is necessary to profile the entire blend run in order to determine or establish any significant deviations in performance when the respective transforms are applied. Clearly the most definitive way to establish whether the application of a pre-processing technique removes relevant information or not is to compare the technique with a reference method. In this paper we are focusing only on qualitative modes of analysis and will not consider a reference technique which will be the focus of part III of this series of work. The resultant profile of the blending process will be dependent on both the pre-processing transform used as well as the wavelength range taken into consideration. Given the obvious noise content of the spectra that results after the second derivative transformation (15 point), it is not likely that a combination of full spectral range and second derivative transform will provide optimum blend profiles.

Once again using Blend # 20 as a typical target blend, the mean standard deviation calculation was used to compare the blend profiles obtained with the various transformations. Fig. 8 shows the profiles that are obtained by using the entire wavelength range of 1100–2500 nm. Here, the resultant mean standard deviation is plotted against the total process time in seconds with the vertical line at 300 s indicating the screening portion of the process which divides blending phases I and II. Similar profiles are obtained with all the transformations used, that is, higher standard deviations are obtained at the start of the blending process and in all cases there appears to be a more stable mean after the screening step. This may suggest that Phase II of the blending protocol is unnecessary. However, note that there is still some variability in the mean standard deviation obtained during Phase II, especially with the second derivative transform (part (d)).

The second approach is to calculate the dissimilarity of the blend spectra with respect to specified time points at which the blend is considered to be homogeneous. The time points provided for this exercise were 1620, 1740 and 1860 s. Although not the last three time points, they appear to be well within a homogenous range as far as could be established. The resultant blend profiles are shown in Fig. 9, with the calculations encompassing the entire wavelength range of 1100–2500 nm. Similar blend profiles to those observed with the mean standard deviation calculations are obtained for all the transforms except the second derivative. This is typical of the case when too much noise is incorporated through the second derivative transform as was done in this case with the inclusion of the entire spectral range. One of the potential advantages of the dissimilarity type of approach to blend profiling is that the calculation can be performed for each of the spectra collected during the run so that a visual evaluation of the extent of scatter of individual readings may be obtained.

Taking this approach a step further, one can calculate the dissimilarity of spectra compared to the individual pure component spectra as opposed to a pre-defined time point(s). In this way it may be possible to discern which components are more homogenous than others. Fig. 10 shows the split plot of dissimilarity values calculated with respect to the four blend components Avicel, Active, DCP and Explotab. Dissimilarity values range from a minimum of 0, which indicates that a spectrum is identical to the target spectrum, i.e. there is no dissimilarity between the two, while the maximum value of 1 indicates that there is no similarity between a spectrum and the target component spectrum. In Fig. 10, the calculations were carried out on raw spectral data using the entire wavelength range. The typical blend profiles are observed, although the dissimilarity numbers plotted on the y-axis should

only be used as a guide and not an absolute indication of similarity. Once again the observation is made that the majority of the mixing is accomplished prior to the screening step.

Taking into consideration the noise contributions observed with the second derivative in the 2300–2500 nm range, the obvious manner in which to minimise this contribution is to restrict the range to a relatively noise-free but information rich region of the spectral domain. Although the noise is more obvious with the second derivative transform, it is present in all other cases as it is an intrinsic part of the manner in which the data was collected and results primarily from the light attenuation through the optic fibres. Restricting the spectral range to that of 1500–1800 nm, the above calculations were repeated for Blend # 20. Fig. 11 shows the blend profiles using the mean standard deviation calculations and Fig. 12 shows the dissimilarity with respect to a homogeneous mixture at times 1620, 1740 and 1860 s. All the standard deviation results provide a similar blend profile. In this case the variability has been reduced for the profile resulting from the second derivative transform. Refer to Fig. 9(d) and Fig. 12(d) for a comparison of the profiles obtained with the second derivative transform over the two spectral regions. Once again the blend appears to have reached homogeneity by the end of Phase I of the blending process. For the dissimilarity calculations shown in Fig. 12, similar conclusions may be reached with all the transforms.

One additional comparison was carried out for the transforms, shown in Fig. 13, whereby the dissimilarity with respect to the pure component spectra was calculated over the wavelength range 1500–1800 nm. The usual blend profiles are observed for all treatments. An interesting observation was made with the second derivative transform (see Fig. 13(d) which shows the split plot of the individual dissimilarity calculations) with respect to the DCP component. Calcium Phosphate anhydrous dibasic is an inorganic compound that does not have a very strong NIR signature, as can be seen in Fig. 4. Using the second derivative transform on this type of spectrum only serves to exaggerate the noise contributions, which are then carried through into the dissimilarity calculations. Note that the extent of variability of the other components is pretty constant so when dealing with this type of compounds one of the other transforms would be recommended.

The consistent observation that can be made with all the transforms and blend profiles obtained in this study is that the majority of the mixing appears to be accomplished during Phase I of the process. Slight variability of the profiles is observed for data collected over Phase II, however one of the more difficult tasks is to establish the significance of that variability. How large does the variance have to be in order to indicate a significant demixing of the blender contents? What level of variability in the calculated criterion represents a normal level of profile deviation? These questions are not easily answered prior to the commencement of a blending run.

Moving onto the PCA approach to blend profiling, Blend # 20 was decomposed and the scores plot is shown in Fig. 14 in a projection defined by the first three principal components. The figure is the result of a second derivative transform (15 point Savitzky-Golay) over the wavelength range 1100-2300 nm and clearly shows the initial four stratified spectra, followed by two clusters. One cluster represents the prescreen or Phase I data collected, while the post screen cluster is the data collected during Phase II of the process. This is consistent with the previous graphical representations of the blend profiles in that clear distinctions are obvious in the two phases. This difference is increased by the milling/screening combination which changes the particle size distribution of the blender contents and is still contributing to the profiles even after the corrective transforms. Another way of profiling the blending process is to simply plot the first score vector obtained in the PCA against the scan or sample number as is shown in Fig. 15. This too appears to be consistent with previous visualisations of the blend profiles in which the majority of the mixing is completed prior to the screen step.

For the next PCA decomposition, ten scans of each of the individual components were decomposed to obtain the loadings vectors, after which the final ten spectra collected for each of the replicate target blends were projected into the same space. Fig. 16 shows the results of this PCA decomposition and projections described by the first three principal components. The wavelength range used was 1500–1800 nm and a second derivative transform (15 point Savitzky-Golay). Only one general observation can be made qualitatively and that is that the target region containing the replicate blend experiments is located in approximately the appropriate location of the tetrahedron. It may be possible to gain more information from quantitative approaches which will be examined at a later date.

Given that four blends were monitored with the same target composition it was possible to evaluate the reproducibility of blend runs. Also it was possible to test the theory that if data on one blend run was available, could it be used for all future blend determinations of the same target composition. First, the last ten collected spectra from the four target runs were merged and a PCA decomposition was carried out using the same second derivative and a wavelength range of 1500–1800 nm. Fig. 17 shows the three dimensional scores plot that results. The ovals have been provided by the authors to enhance interpretation and to make even more obvious the resultant groupings. Clearly, some batch to batch differences do exist, however it should be noted that the PCA algorithm serves to enhance differences present in the data. Also, from a scores plot such as this, it is almost impossible to obtain a level of significance of these differences. In order to obtain an estimate of the level of significance of the replicate differences observed, a PCA decomposition was carried out on the spectral data collected for the four replicate runs together with Blend # 1 and Blend # 10. These two blends have different compositions than the replicates and should therefore provide a yardstick for the observed differences. Fig. 18 shows the resultant scores plot which shows that the difference between the different compositions are larger than those between the replicate runs, which can no longer be distinguished from each other. Similar results are obtained with other transforms.

Another way of evaluating the significance of the observed cluster differences is to construct a SIMCA model on data collected for one of the batches and use that model to predict the responses of the other blend runs. A model was generated for Blend # 20 using the second derivative over the wavelength range 1500–1800 nm. The model was then used to predict the last ten scans of the four target blend runs. The results of this prediction are shown in Fig. 19, where the horizontal line indicates the model threshold established at a confidence level of 99%. Note that only one of the scans was rejected by the constructed model which is consistent with the specified probability threshold ($P = 0.99$). Comparing this with a prediction of an entire blender run, Blend # 19 is used to generate the plot in Fig. 20, it is seen that the spectra collected during Phase I of the blending process are rejected by the model and that the later scans are correctly identified as being of the target composition. The conclusion can therefore be made that for this target blend, the data collected during one blend run can be used to appropriately evaluate the blend homogeneity of other blending runs with the same target composition.

Given that most pharmaceutical applications and test methods have a suitable range of operability which are provided by the product specifications, and also given that it was shown above that one blend run is comparable to another, the next qualitative investigation was focused on the ability of a SIMCA model to evaluate if blend data was within specification or not. To accomplish this, the Active blends covering the range of 95–105% of target formulation were merged and used to construct a SIMCA model. The spectral data was over the wavelength range 1500–1800 nm was transformed using a second derivative (15 point smooth, 21 point derivative) and a model was constructed using five principal components. The remaining blend runs, 85 and 115% of target formulation, were then used to test the constructed model. Fig. 21 is the resultant SIMCA

prediction distance plot which shows the distances calculated for the data used to construct the model (to the left of the dashed line and below the solid horizontal line indicating the model threshold) and the additional data used to challenge the model (located to the right of the dashed vertical line). The probability level for the figure shown is 0.85, and this parameter can be further adjusted to fine-tune the threshold.

The model was able to distinguish between the within specification blends and those that would be considered to be outside the stated specification of 95–105% of target formulation. One problem blend was discovered (circled in Fig. 21) which was Blend # 9, which upon investigation was determined to have had the wrong amount of Active added to the blender. Instead of the expected amount of 4% indicated by the experimental design, 3.33% was added. The actual level is within the model range of 95–105% of target and therefore should be passed by the model. Note that due to the addition of a different amount of Active, the proportions of all the other components are different to those in the experience set and thus some of the scans are also failed. This is an example of both the advantage and disadvantage of a sample matrix interrogation approach technique such as NIR spectroscopy. On the one hand the method was able to respond appropriately by passing the problem batch, while on the other it flagged that it was a problem blend thus initiating a closer look at that run. Overall, the conclusion can be made that construction of SIMCA models to determine if blend compositions are within a given specification range are a feasible approach.

5. Conclusions

This communication has attempted to highlight some of the concepts involved with blend homogeneity determinations in a pharmaceutical industry application. The designed experiments have been used to generate a sufficient amount of spectral data which was used here to evaluate the utility of a variety of approaches to spectral transformation and blend profiling. The consistency of the blend profiles obtained here did not aid inestablishing any advantages in using one transform over another however is was noted that using the second derivative Savitsky-Golay transformation appeared to be more sensitive to noise. Similarly the blend profiling approaches used here did not show any appreciable differences. Clearly care does need to be taken when contemplating this type of work in that the combination of transform and blend profile criterion should be compatible (for example, the second derivative observation made here). It was shown that with the construction of a SIMCA model on data collected at the end point of one of the blend runs, it was possible to predict a similar end point for additional runs of the same composition. This indicates that if it can be shown that the scale of the blending process is not significant, it would be possible to use a small scale synthetic blend of the target composition to construct a profile or homogeneity end point model which can then be used for real scale blending operations. This will need to be experimentally established at a future time. Additional insight may be obtained when the quantitative approaches are examined for blend evaluation.

Acknowledgements

The authors would like to thank F. Cuesta Sanchez for providing the Matlab mixture analysis code used for some of this work, Tony Toms for helpful discussions and Graham Napier for coordination of supplies and helpful advice throughout the project.

References

[1] R.E. Schirmer, Modern Methods of Pharmaceutical Analysis, 2nd ed., chap. 3, CRC Press, Boca Raton, FL, 1991, pp. 127–170.
[2] R.A. Lodder, G. Hieftje, Appl. Spec. 42 (1988) 4.
[3] P.K. Aldridge, R.F. Mushinsky, M.M. Andino, C.L. Evans, Appl. Spec. 48 10 (1994) 1272.

[4] E.W. Ciurczak, Pharm. Tech. September (1991).
[5] P.A. Hailey, P. Doherty, P. Tapsell, T. Oliver, P.K. Aldridge, J. Pharm. Biomed. Anal. 14 (1996) 551–559.
[6] S.S. Sekulic, H.W. Ward II, D.R. Brannegan, E.D. Stanley, C.L. Evans, S.T. Sciavolino, P.A. Hailey, P.K. Aldridge, Anal. Chem. 68 (3) (1996) 509–513.
[7] F. Cuesta Sanchez, J. Toft, B. van den Bogaert, D.L. Massart, S.S. Dive, P.A. Hailey, Fresnius J. Anal. Chem. 352 (1995) 771–778.
[8] V.W. Uhl, J.B. Gray, Mixing: Theory and Practice, Academic Press, New York, 1967.
[9] H.C. Ansel, N.G. Popovich, Pharmaceutical Dosage Forms and Drug Delivery Systems, 5th ed., Lea and Febiger, Philadelphia, PA, 1990, pp. 134–195.
[10] R.J. Barnes, M.S. Dhanoa, S.J. Lister, Appl. Spec. 43 (1989) 772–777.
[11] A. Savitzky, M.J.E. Golay, Anal. Chem. 36 (1964) 1627–1639.
[12] F. Cuesta Sanchez, M.S. Khots, D.L. Massart, Anal. Chim. Acta 290 (1994) 249–258.
[13] H.H. Harmon, Modern Factor Analysis, University of Chicago Press, Chicago, IL, 1976, Chapter 12-1.